

## X-ray studies on the interaction of the antimicrobial peptide gramicidin S with microbial lipid extracts: evidence for cubic phase formation

Erich Staudegger<sup>a</sup>, Elmar J. Prenner<sup>b</sup>, Manfred Kriechbaum<sup>a</sup>, Gábor Degovics<sup>a</sup>, Ruthven N.A.H. Lewis<sup>b</sup>, Ronald N. McElhaney<sup>b</sup>, Karl Lohner<sup>a,\*</sup>

<sup>a</sup> *Institut für Biophysik und Röntgenstrukturforschung, Österreichische Akademie der Wissenschaften, Steyergasse 17/VI, A-8010 Graz, Austria*

<sup>b</sup> *Department of Biochemistry, University of Alberta, Edmonton, AB, Canada T6G 2H7*

Received 21 March 2000; received in revised form 29 May 2000; accepted 7 June 2000

### Abstract

We have investigated the effect of the interaction of the antimicrobial peptide gramicidin S (GS) on the thermotropic phase behavior of model lipid bilayer membranes generated from the total membrane lipids of *Acholeplasma laidlawii* B and *Escherichia coli*. The *A. laidlawii* B membrane lipids consist primarily of neutral glycolipids and anionic phospholipids, while the *E. coli* inner membrane lipids consist exclusively of zwitterionic and anionic phospholipids. We show that the addition of GS at a lipid-to-peptide molar ratio of 25 strongly promotes the formation of bicontinuous inverted cubic phases in both of these lipid model membranes, predominantly of space group Pn3m. In addition, the presence of GS causes a thinning of the liquid-crystalline bilayer and a reduction in the lattice spacing of the inverted cubic phase which can form in the GS-free membrane lipid extracts at sufficiently high temperatures. This latter finding implies that GS potentiates the formation of an inverted cubic phase by increasing the negative curvature stress in the host lipid bilayer. This effect may be an important aspect of the permeabilization and eventual disruption of the lipid bilayer phase of biological membranes, which appears to be the mechanism by which GS kills bacterial cells and lysis erythrocytes. © 2000 Elsevier Science B.V. All rights reserved.

**Keywords:** Gramicidin S; Antimicrobial peptide; Phospholipid; Microbial lipid; Lipid–peptide interaction; Non-lamellar phase

### 1. Introduction

Gramicidin S (GS) is a cyclic decapeptide of primary structure (cyclo-(Val-Orn-Leu-D-Phe-Pro)<sub>2</sub>) (see Fig. 1) first isolated from *Bacillus brevis* [1]. This peptide shows potent antibiotic activity against a broad spectrum of both Gram-negative and Gram-positive bacteria as well as several pathogenic fungi

(see [2–5]). Unfortunately, GS is rather non-specific in its actions and exhibits appreciable hemolytic as well as antimicrobial activity, thus restricting the use of GS as an antibiotic to topical applications (see [2,3]). However, recent work has shown that structural analogs of GS can be designed with markedly reduced hemolytic activity and enhanced antimicrobial activity, suggesting the possibility that appropriate GS derivatives may be used as potent oral or injectable broad-spectrum antibiotics [4,5].

GS has been extensively studied by a wide range of physical techniques (see [2,3]) and its three-dimensional structure is shown in Fig. 1. In this minimum

\* Corresponding author. Fax: +43-316-812367;  
E-mail: karl.lohner@oeaw.ac.at

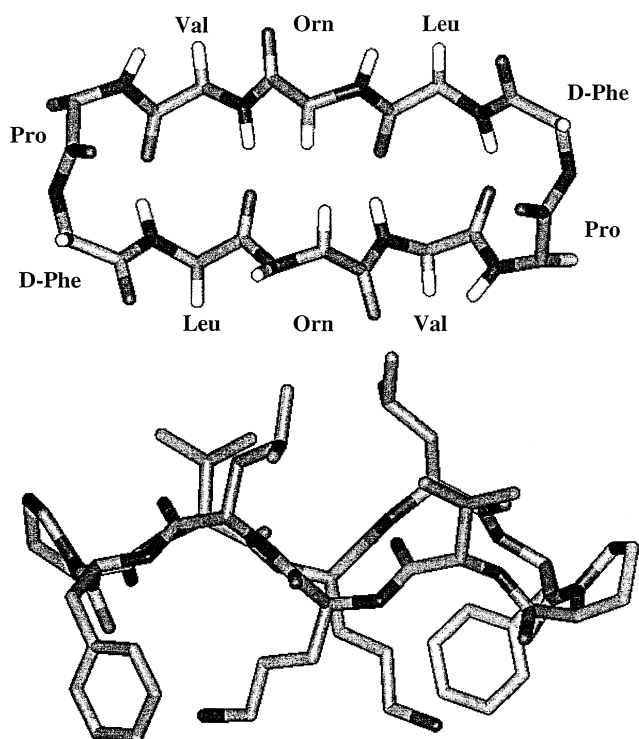


Fig. 1. The structure and conformation of GS. The upper panel is a view of the GS molecule perpendicular to the plane of the ring, illustrating the peptide backbone structure and the positions of the hydrogen bonds in the antiparallel  $\beta$ -sheet region. The lower panel is a view of the GS molecule in the plane of the ring, indicating the disposition in space of the hydrophobic Val and Leu residues (top) and the basic Orn residues (bottom) relative to the peptide ring.

energy conformation, the two tripeptide sequences Val-Orn-Leu form an antiparallel  $\beta$ -sheet terminated on each side by a type II'  $\beta$ -turn formed by the two D-Phe-Pro sequences. Four intramolecular hydrogen bonds, involving the amide protons and carbonyl groups of the two Leu and two Val residues, stabilize this rather rigid structure. Note that the GS molecule is amphiphilic, with the two polar and positively charged Orn side chains and the two D-Phe rings projecting from one side of this molecule, and the four hydrophobic Leu and Val side chain projecting from the other side. Moreover, the amphiphilic nature of GS is crucial for the manifestation of its antimicrobial activity [6,7]. A number of studies have shown that this conformation of the GS molecule is maintained in water, in protic and aprotic organic solvents of widely varying polarity, and in detergent micelles and phospholipid bilayers, even

at high temperatures and in the presence of agents which often alter protein conformation (see [2,3]).

Considerable evidence exists that the principal target of GS is the lipid bilayer of bacterial or erythrocyte membranes (see [2,3,8]). Therefore, a number of biophysical studies have been carried out on the effect of GS on the structure and physical properties of phospholipid bilayer model and biological membranes (for a review, see [8]). There is a general consensus that GS partitions strongly into the biologically relevant liquid-crystalline ( $L_{\alpha}$ ) phase of lipid bilayers and is located primarily near the glycerol backbone region of the phospholipid molecule, where it interacts with the lipid polar headgroups and the upper regions of the lipid hydrocarbon chains. The presence of GS seems to further disorder liquid-crystalline bilayers and, at sufficiently high concentrations, may destroy the lipid bilayer structure. The presence of GS at lower concentrations also increases the permeability of model and biological membranes and at higher concentration causes membrane lysis and solubilization. Finally, GS seems to interact more strongly with anionic than with zwitterionic or uncharged phospho- or glycolipid bilayers and the interaction of GS with these model membranes is reduced by the presence of cholesterol [8].

We have recently shown that GS can also alter the lamellar/non-lamellar phase preferences of some phospholipid and glycolipid molecular species [9]. Specifically, we examined the interactions of GS (lipid/peptide ratio 25:1) with a variety of single-component lipid bilayers, and with membrane polar lipid extracts of *Acholeplasma laidlawii* B and *Escherichia coli*, by  $^{31}\text{P}$ -NMR spectroscopy and X-ray diffraction. For mixtures of GS with lipids such as phosphatidylcholine (PC), phosphatidylserine (PS), cardiolipin, and sphingomyelin, axially symmetric  $^{31}\text{P}$ -NMR lamellar phase powder patterns are observed throughout the entire temperature range examined (0–90°C). However, with mixtures of GS with either phosphatidylethanolamine (PE), phosphatidylglycerol (PG), or a non-lamellar phase-forming phosphatidylcholine, axially symmetric  $^{31}\text{P}$ -NMR powder patterns are also observed at low temperatures. However, at high temperatures, an isotropic component is observed in their  $^{31}\text{P}$ -NMR spectra, and the relative intensity of this component increases signifi-

cantly with temperature and with GS concentration. Once formed at high temperatures, this isotropic component exhibits a marked cooling hysteresis and in most cases disappears only when the sample is recooled to temperatures well below the lipid hydrocarbon chain-melting phase transition temperature. We also showed that GS induces the formation of isotropic components in the  $^{31}\text{P}$ -NMR spectra of heterogeneous lipid mixtures such as occur in *A. laidlawii* B and *E. coli* membranes. These observations suggest that GS induces the formation of cubic (Q) or other three-dimensionally ordered inverted non-lamellar phases when it interacts with some types of lipid bilayers, a suggestion strongly supported by our X-ray diffraction studies. Moreover, we found that the capacity of GS to induce the formation of such phases increases with the intrinsic non-lamellar phase-preferring tendencies of the lipids with which it interacts.

The appearance of an isotropic signal in the  $^{31}\text{P}$ -NMR spectrum of aqueous phospholipid dispersions is observed for fast tumbling lipid aggregates, like small unilamellar vesicles and micelles, or for Q or other three dimensionally ordered inverted non-lamellar phases. As  $^{31}\text{P}$ -NMR spectroscopy cannot distinguish between these putative lipid-peptide aggregates due to their fast tumbling in respect to the  $^{31}\text{P}$ -NMR time scale (e.g. [10,11]), these lipid aggregates were further studied by X-ray techniques. Prenner et al. [9] found that isotropic  $^{31}\text{P}$ -NMR spectra are observed at high temperatures. Moreover, a mixture of dimyristoylphosphatidylethanolamine-GS, exhibited very weak reflections in addition to strong lamellar Bragg reflections at temperatures higher than 85°C. The probable existence of an inverted Q phase in the form of two gyroid lattices with a basis of 13.1 and 15.3 nm were proposed from these supplementary reflections, which could not be indexed on a lamellar phase. Thus in order to obtain information on the structural basis of the isotropic component of lipid extracts from the plasma membranes of *E. coli* and *A. laidlawii* B, we performed a much more extensive X-ray diffraction study. We clearly show here that the interaction of GS with these lipid extracts from natural bacterial membranes markedly enhances their tendencies to form non-lamellar isotropic phases, which could be identified as a bicontinuous cubic lipid phase.

## 2. Materials and methods

### 2.1. Peptides and lipids

The cyclic peptide gramicidin S (HCl salt) was obtained from Sigma (St. Louis, MO) and purified by the HPLC methodology described by Kondejewski et al. [4]. The *A. laidlawii* B membrane lipids used were the polar lipid extracts of cells grown in avidin-containing media supplemented with an equimolar mixture of palmitic and oleic acid. The polar lipid extracts were obtained by silicic acid chromatography of the total membrane lipid extracts [12]. *E. coli* total and polar lipid extracts were obtained from Avanti Polar Lipids (Alabaster, AL).

### 2.2. Sample preparation

Lipid-peptide mixtures (lipid-peptide molar ratio,  $R=25$ ) were prepared in glass tubes by codissolving the lipid extracts in chloroform/methanol (2:1 v/v) with appropriate amounts of GS stock solutions (chloroform/methanol 1:2 v/v) and subsequent evaporation of the solvent under a stream of nitrogen. After removal of any residual traces of solvent in vacuo overnight, the dried lipid or lipid-peptide films were hydrated by vigorous vortexing at 40°C with a buffer consisting of 50 mM Tris, 100 mM NaCl, 5 mM EDTA and 1 mM sodium azide (pH 7.4). The lipid concentration of the X-ray samples was 5–10 mg/100  $\mu\text{l}$ .

### 2.3. Small- and wide-angle X-ray (SWAX) experiments

SWAX diffraction experiments were performed on a modified Kratky compact camera (HECUS-MBraun-Graz, Graz, Austria), which allows simultaneous recording of diffraction data in both the small- and wide-angle region, as described elsewhere [13]. Ni-filtered  $\text{CuK}\alpha$ -radiation ( $\lambda=0.154$  nm) originating from a Philips X-ray generator with a Cu-anode operating at 50 kV and 40 mA was used. The camera was equipped with a Peltier-controlled, variable-temperature cuvette (temperature precision =  $\pm 0.1^\circ\text{C}$ ) and linear, one-dimensional, position-sensitive detectors OED 50-M (MBraun, Garching, Germany). Calibration in the small-angle region was performed

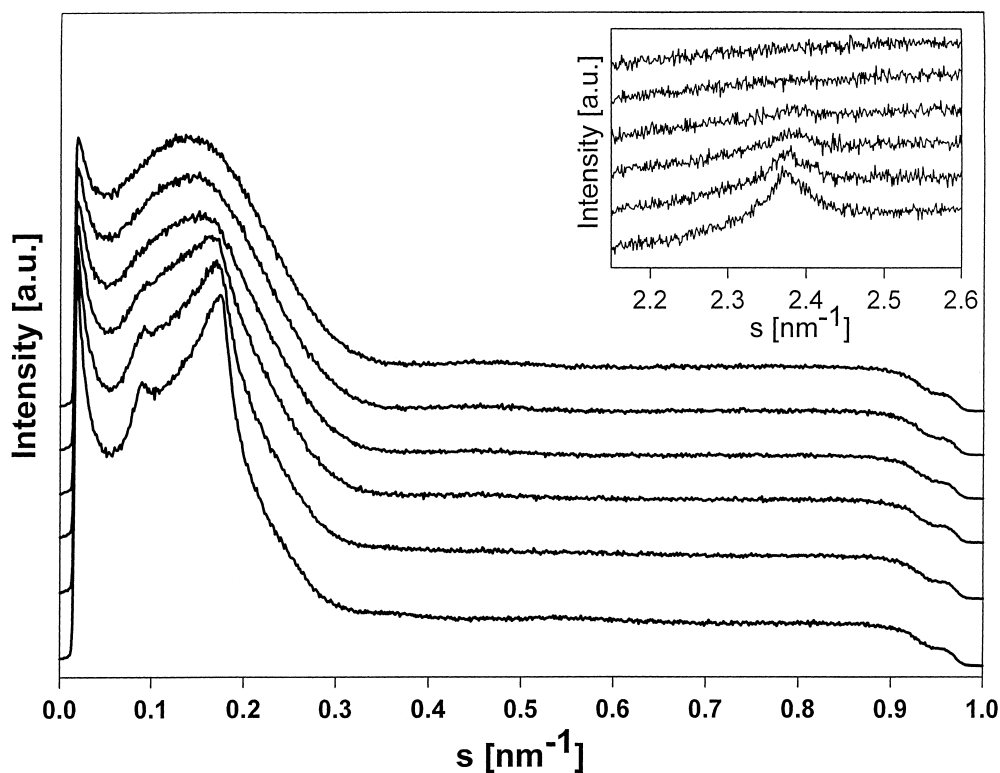


Fig. 2. Small- and wide-angle (inset) X-ray diffractograms of an aqueous dispersion of *A. laidlawii* B membrane polar lipid extract recorded at 5, 10, 15, 20, 25 and 30°C (bottom to top);  $s = 1/d = 2\sin(\Theta)/\lambda$ , where  $\lambda$  is the wavelength of the X-ray beam and  $2\Theta$  the scattering angle. Diffractograms are displayed vertically for better visualization.

with silver stearate and in the wide-angle region with *p*-bromo-benzoic acid standards, respectively. Temperature control and data acquisition was achieved by programmable temperature control equipment (MTC-2.0, HECUS-MBraun-Graz, Graz, Austria). A temperature cycle consisted of a ramp from 25 to 90°C and then back to 25°C in steps of 5°C. The samples were equilibrated at the respective temperatures for 10 min before sampling the X-ray diffractograms. Multiplexed exposure times of 2000 s for the small-angle and 1000 s for the wide-angle region were chosen.

Synchrotrone X-ray measurements were performed at the high-flux Austrian SAXS beamline (station 5.2L) of the 2 GeV electron storage ring ELETTRA, Trieste [14] using the 8-keV X-rays which corresponds to a wavelength of 0.1542 nm. The samples were placed in Mark glass capillaries with a diameter of 1 mm, sealed and mounted in a rotating sample stage. The resolution range was from 20 to 2 nm and exposure times of 120 s were chosen. Diffractograms

were recorded by means of a linear position-sensitive detector. While the rectangular slit geometry, defining the profile of the beam, of the SWAX camera in the laboratory yields X-ray diffraction pattern convoluted with the beam profile, this effect is negligible at the SAXS beamline at ELETTRA.

SAXS-data arising from particle scattering were further analyzed by Indirect Fourier Transformation. In the case of flat particles, such as extended lamellar structures, where the axial thickness of the lamella is much smaller than its surface area, the one-dimensional distance distribution function  $p_t(r)$  can be derived from the scattering data. This represents the autocorrelation function of the electron density normal to the bilayer plane, which yields information on the cross-bilayer distance between the electron-dense phosphate groups ( $d_{p-p}$ ), i.e. of the phosphate groups located in the opposing monolayers of the bilayer. Thereby,  $d_{p-p}$  can be determined from the position of the outer maximum of the  $p_t(r)$ -function (see also Fig. 4a). Briefly,  $p_t(r)$  were computed after

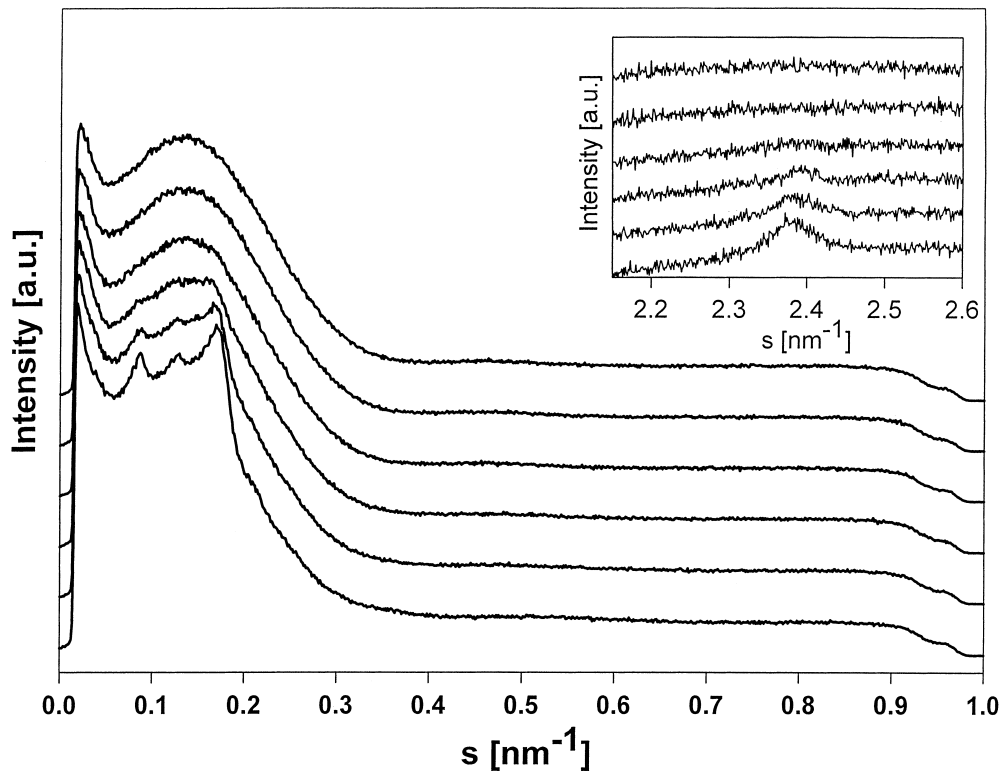


Fig. 3. Small- and wide-angle (inset) X-ray diffractograms of an aqueous dispersion of a mixture of *A. laidlawii* B membrane polar lipid extract and GS at a lipid-to-peptide molar ratio of 25:1 recorded at 5, 10, 15, 20, 25 and 30°C (bottom to top);  $s = 1/d = 2\sin(\Theta)/\lambda$ , where  $\lambda$  is the wavelength of the X-ray beam and  $2\Theta$  the scattering angle. Diffractograms are displayed vertically for better visualization.

background subtraction and normalization of the respective buffer blank curve and data-point reduction of the difference curve by a funneling routine. Furthermore, the data were corrected for instrumental broadening by using the program ITP of Glatter [15] to yield desmeared data, which were interpreted in real space in terms of their pair distance distribution function [16,17].

### 3. Results

*A. laidlawii* B membrane lipid dispersions. Representative SWAX diffraction patterns for aqueous dispersions of the membrane polar lipids derived from *A. laidlawii* B are shown in Fig. 2. At temperatures between 5 and 15°C, the wide-angle diffractograms exhibit a single symmetric peak centered at 0.42 nm ( $s = 2.38 \text{ nm}^{-1}$ ), whose scattering intensity decreases with increasing temperature, vanishing around 20°C

(inset Fig. 2). Such a diffraction pattern is characteristic of hexagonally packed all-*trans* lipid acyl chains oriented normal to the bilayer plane as observed for the lamellar gel ( $L_{\beta}$ ) phase [18]. At temperatures above 20°C, only a diffuse pattern is detected, which demonstrates that all the lipid hydrocarbon chains are in a melted state, characteristic of the lamellar liquid-crystalline ( $L_{\alpha}$ ) phase. This  $L_{\beta}$  to  $L_{\alpha}$  phase transition is also reflected in the small-angle X-ray experiments (Fig. 2). Below 20°C, these diffractograms show two clearly resolvable reflections superimposed upon a broad scattering background, while at 25°C, the diffraction pattern is characterized by broad side maxima and minima. Moreover, a strong scattering intensity in the innermost part, i.e. at very low angles ( $s < 0.05 \text{ nm}^{-1}$ ), typical for particle scattering, is observed in this temperature range. This latter feature suggests the existence of unilamellar vesicles, most likely resulting from the high content of negatively charged lipids in this microbial lipid

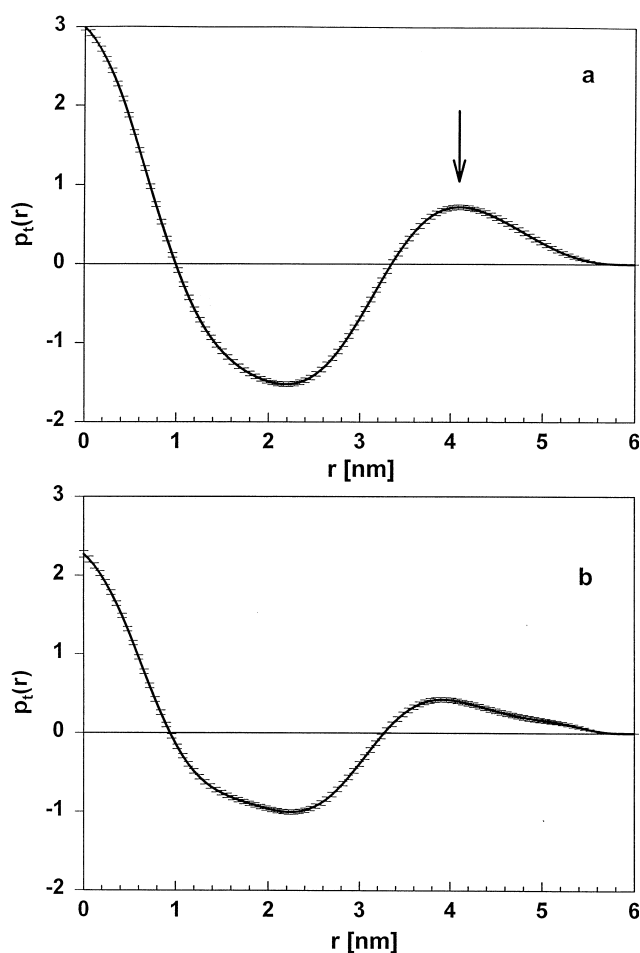


Fig. 4. Computed one-dimensional thickness distance distribution function  $p_i(r)$  of *A. laidlawii* B membrane polar lipid extract (a) and mixtures of these lipids with GS at a lipid-to-peptide molar ratio of 25:1 (b) derived from experimental scattering data at 25°C. Arrow in the upper panel indicates  $d_{P-P}$ ; for details see Section 2.

extract. On the other hand, the presence of two reflections may be attributed to first- and second-order Bragg reflections of a lamellar lattice of 11.3 nm, which suggests the existence of multilamellar vesicles as well. However, the broad reflections are indicative that these liposomes have only a small number of lamellae [19] and/or exhibit a strong distortion of the long range order of the lattice [20]. In this temperature range, generally similar SWAX diffraction patterns were obtained for mixtures of the *A. laidlawii* B membrane polar lipids with GS ( $R=25$ ) (Fig. 3). However, a closer inspection of the wide-angle diffractograms (inset Fig. 3) reveals a slightly smaller ( $\sim 15\%$ ) integral peak intensity below 20°C as com-

pared to the integral peak intensities of the polar lipids without GS. However, the peak position is not affected. This is indicative of partially perturbed hydrocarbon side chains, suggesting an interaction of the peptide with some fraction of the lipids. Additionally, in the small-angle region of the GS-containing sample (Fig. 3), a third Bragg reflection is observed at 7.1 nm ( $s=0.14 \text{ nm}^{-1}$ ), residing between the two reflections which are characteristic for the *A. laidlawii* B lipid extract, also indicating an interaction of the peptide with this lipid extract below the lamellar gel to liquid-crystalline phase transition region. The limited number of Bragg reflections did not allow any assignment of a non-lamellar phase. On the other hand, these three Bragg reflections cannot be attributed to one single lamellar phase either. As we are dealing with a complex lipid mixture here, the additional reflection could arise from a stronger interaction of GS with the negatively charged lipids present [8], which may give rise to a new lamellar structure.

Information on the cross-bilayer distance between the electron dense phosphate groups of the opposing lipid leaflets was derived from the one-dimensional distance distribution function  $p_i(r)$  as described in Section 2. Such functions are shown in Fig. 4 for lipid extracts of *A. laidlawii* B in the absence (panel a) and in the presence (panel b) of GS at 25°C. We find that in the presence of GS,  $d_{P-P}$  is reduced significantly by about 0.25 nm in the presence of the peptide, i.e. from 4.1 to 3.85 nm. Moreover, in the presence of GS, the outer maximum exhibits an asymmetry towards larger distances as well as a shoulder around 5.3 nm, which may be due to peptide being bound to the membrane surface.

Heating aqueous dispersions of *A. laidlawii* B membrane polar lipids up to 90°C reveals a second phase transition centered around 70°C (Fig. 5a). Above 35°C the scattering intensity in the innermost part of the diffractogram ( $s < 0.05 \text{ nm}^{-1}$ ), as well as the intensity of the broad side maxima, decreases drastically. Concomitantly, the formation of Bragg reflections is observed being superimposed upon the side maximum around 7 nm ( $s=0.143 \text{ nm}^{-1}$ ). These additional peaks increase in intensity with increasing temperature. This higher temperature phase shows a strong hysteresis upon subsequent cooling to 25°C and is stable upon repeated heating and cooling

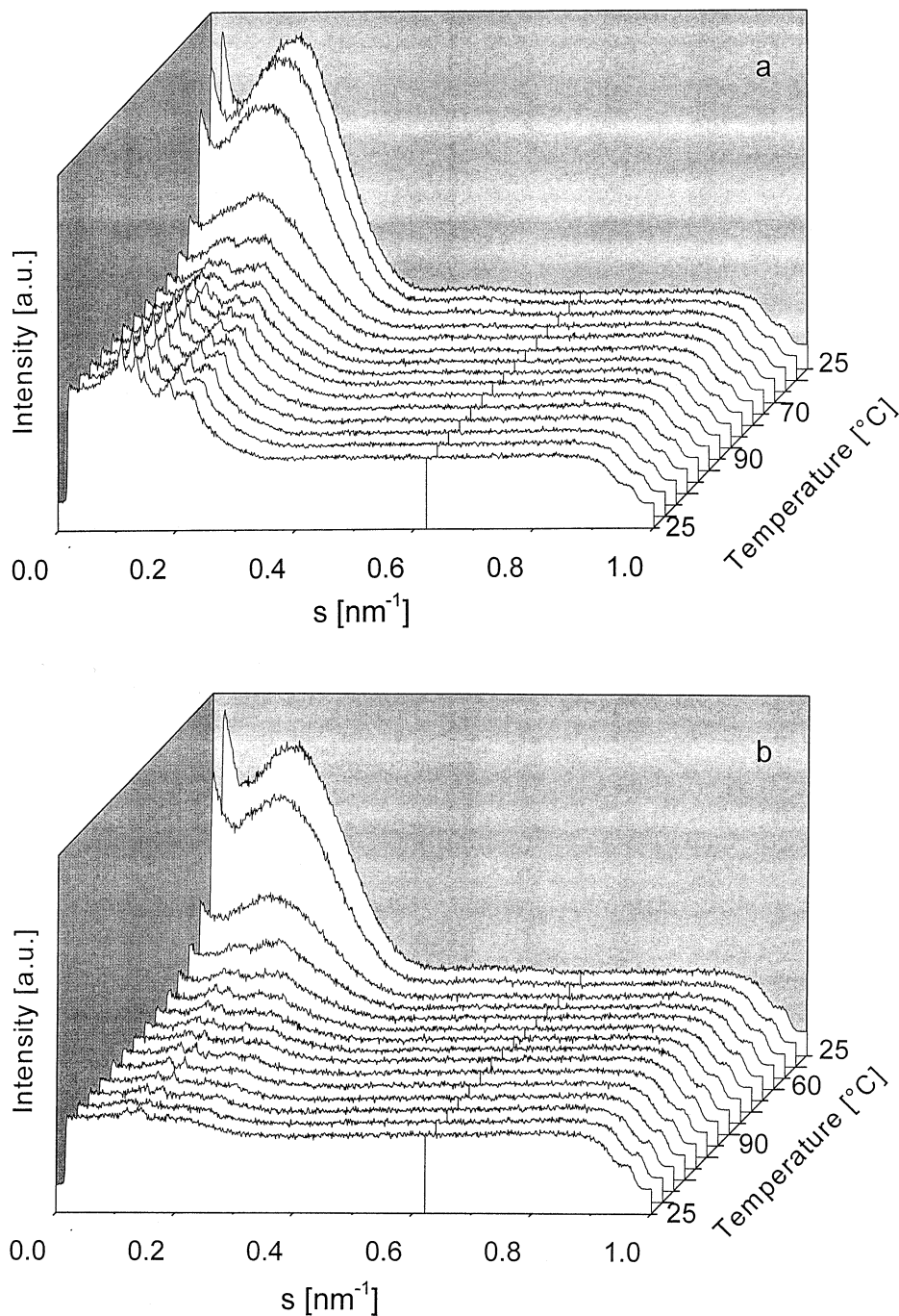


Fig. 5. Small-angle X-ray diffractograms of an aqueous dispersion of *A. laidlawii* B membrane polar lipid extract (a) and a mixture of these lipids with GS at a lipid-to-peptide molar ratio of 25:1 (b) recorded from the first heating and cooling cycle (frames from top to bottom: 25, 35, 45, 60, 70, 75, 80, 85, 90, 80, 70, 60, 50, 40, 25°C; selected temperatures are indicated in the panels);  $s = 1/d = 2\sin(\theta)/\lambda$ , where  $\lambda$  is the wavelength of the X-ray beam and  $2\theta$  the scattering angle.

cycles, a common feature of three-dimensional isotropic phases. This new supramolecular phase seems to coexist with the lamellar phase under these experimental conditions, as evidenced by the broad back-

ground scattering and by the weak, but still significant, side maxima at higher angles arising from the particle scattering. Our previous <sup>31</sup>P-NMR data also indicated a coexistence of an isotropic phase with a

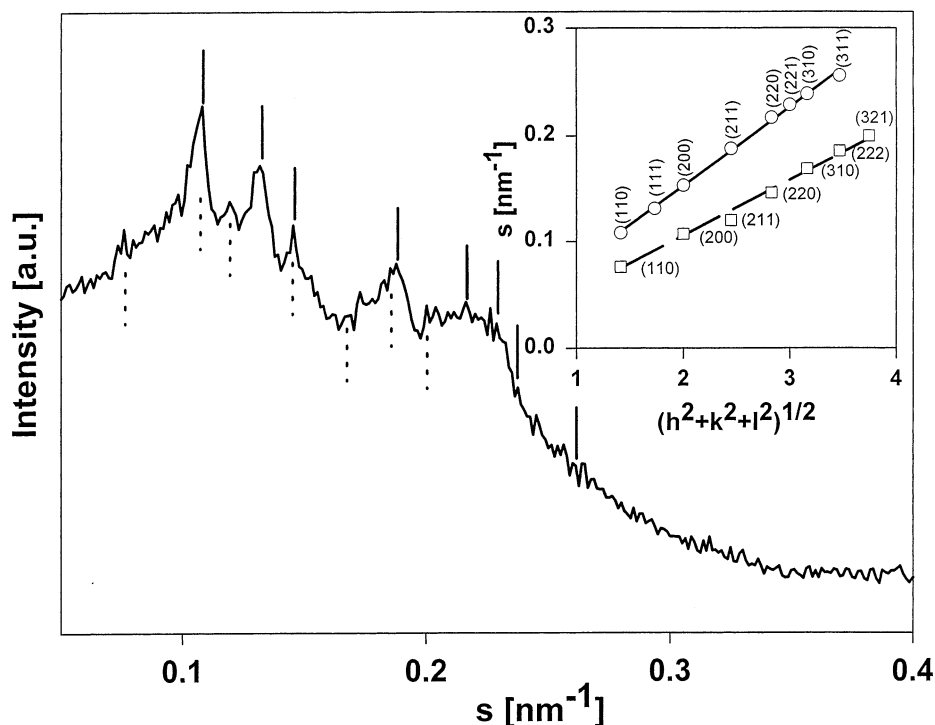


Fig. 6. Phase assignment of an aqueous dispersion of *A. laidlawii* B membrane polar lipid extract. Position of  $hkl$ -reflections corresponding to a cubic phase of space group Pn3m (solid line) and of space group Im3m (broken line), respectively, are indicated in the diffractogram. The inset shows the indexing of these two cubic lattices from the plot  $s$  vs.  $(h^2+k^2+l^2)^{1/2}$ ; open circles represent reflections of space group Pn3m, while open squares represent reflections of space group Im3m. Miller indices ( $hkl$ ) are indicated in the panel. Data were recorded at 25°C after the first heating/cooling cycle up to 90°C.

lamellar one in this same range of temperatures [9]. Sometimes, the resolution of the reflections arising from such phases in the presence of the intrinsically stronger scattering from the lamellar phase can be difficult in a mixed phase system, even when the former is the dominant component in the mixture. However, we were able to unequivocally assign the existence of two cubic phases (Fig. 6). The predominant one consists of up to eight orders of diffraction space in the ratio of  $\sqrt{2}:\sqrt{3}:\sqrt{4}:\sqrt{6}:\sqrt{8}:\sqrt{9}:\sqrt{10}:\sqrt{11}$  which were indexed as (110), (111), (200), (211), (220), (221), (310), and (311) reflections on a three-dimensional cubic phase of space group Pn3m. The reciprocal spacing ( $s$ ) of cubic phases is related to the lattice spacing ( $a$ ) by

$$s(hkl) = (h^2 + k^2 + l^2)^{1/2} / a \quad (1)$$

where  $h$ ,  $k$ , and  $l$  are the Miller indices [21]. Therefore, the lattice spacing can be calculated from the reciprocal gradient of the plot  $s$  vs.  $(h^2+k^2+l^2)^{1/2}$ . From this plot a lattice spacing of 13.2 nm was cal-

culated for the Pn3m phase (see inset Fig. 6). This value is in the same range as previously reported ones (12.5–14 nm) for lipids adopting the Pn3m or Pn3 space group [22]. A second cubic phase can be detected from additional weak reflections which do not belong to the Pn3m space group. These reflections are in ratios of  $\sqrt{2}:\sqrt{4}:\sqrt{6}:\sqrt{8}:\sqrt{10}:\sqrt{12}:\sqrt{14}$ , which were indexed as (110), (200), (211), (220), (310), (222), and (321) reflections on a three-dimensional cubic phase of space group Im3m (inset Fig. 6). A lattice spacing of 18.9 nm was calculated. It should be noted that an assignment of other cubic phases failed. Coexisting Pn3m and Im3m phases were also reported from aqueous dispersions of dioleoylphosphatidylethanolamine (DOPE) which were cycled 1400 times through the  $L_\alpha$ -inverted hexagonal ( $H_{II}$ ) phase transition range [23]. Moreover, for dielaidoyl PE a cooperative Im3m  $\rightarrow$  Pn3m transition was observed at elevated temperatures and transforms the latter phase into a mixture of coexisting Pn3m and Im3m phases [24]. Our results are also in accordance

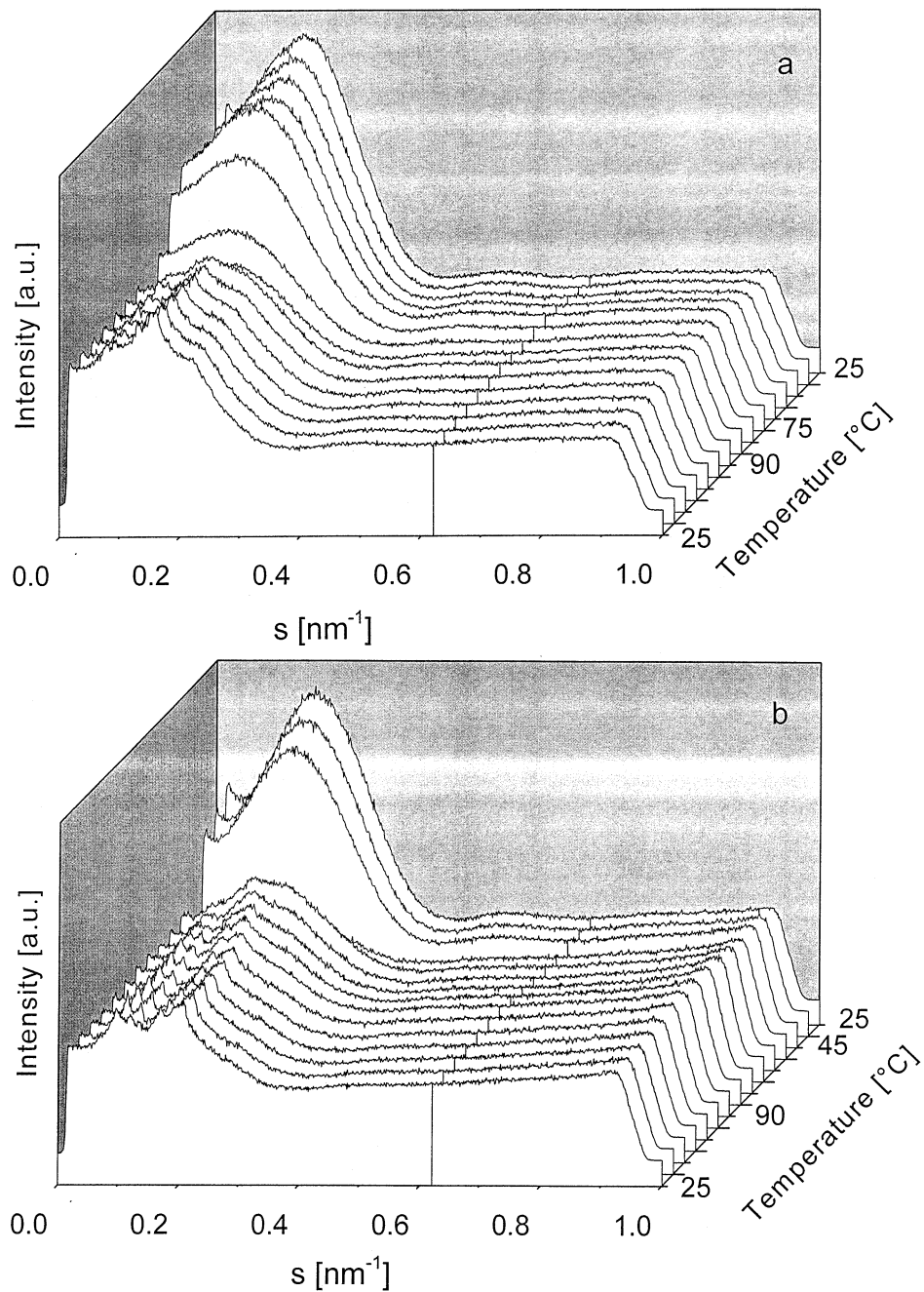


Fig. 7. Small-angle X-ray diffractograms of an aqueous dispersion of *E. coli* membrane polar lipid extract (a) and a mixture of these lipids with GS at a lipid-to-peptide molar ratio of 25:1 (b) recorded from the first heating and cooling cycle (frames from top to bottom: 25, 35, 45, 60, 70, 75, 80, 85, 90, 80, 70, 60, 50, 40, 25°C; selected temperatures are indicated in the panels);  $s$ , see legend to Fig. 5.

with observations by Sen et al. [25], who reported the presence of Pn3m or Pn3 space groups for synthetic monoglucosyldiacylglycerol. Moreover, Lindblom and coworkers [26] recently characterized the phase behavior of single lipid components of *A. laidlawii*

(strain A) by NMR and X-ray diffraction. The strongest non-lamellar propensity was reported for monoglucosyldiacylglycerol and a monoacylmonoglucosyldiacylglycerol derivative, for which a Q phase of the space group Ia3d was assigned at 20 wt% of water in

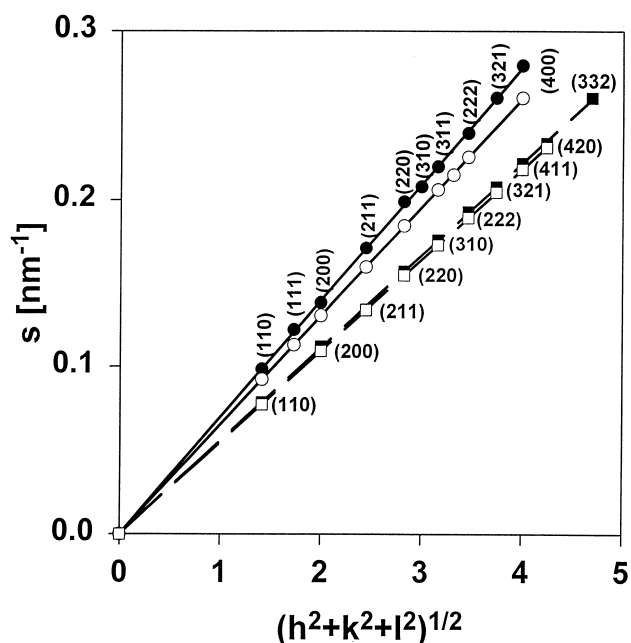


Fig. 8. Phase assignment of an aqueous dispersion of *E. coli* membrane polar lipid extract in the absence and presence of GS at a lipid-to-peptide molar ratio of 25:1. Reflex positions for two cubic lattices vs.  $(h^2+k^2+l^2)^{1/2}$  are shown; circles represent reflections of space group Pn3m, while squares represent reflections of space group Im3m (closed symbols with and open symbols without GS). Miller indices  $(hkl)$  are indicated in the panel. Reflections were taken from diffractograms recorded at 25°C after the first heating/cooling cycle up to 90°C.

the sample. These findings are not in contradiction to our present results, but can be explained by the different levels of hydration studied, as Lindblom and Rilfors [27] presented experimental and theoretical evidence that the sequence of formation of different Q phases with increasing water content is  $Ia3d \rightarrow Pn3m \rightarrow Im3m$ .

Table 1

Lattice spacing of the Pn3m cubic phase for microbial lipid extracts at 25°C after the first heating/cooling cycle<sup>a</sup>

Microbial lipid extract	Gramicidin S ( $R=25$ ) <sup>b</sup>	Lattice spacing (nm)
<i>A. laidlawii</i> B,	–	13.2
polar	+	12.0 <sup>c</sup>
<i>E. coli</i> ,	–	15.3
polar	+	14.3
<i>E. coli</i>	–	14.9
total	+	13.4

<sup>a</sup>A minor fraction of lipids was found to adopt a cubic phase of space group Im3m characterized by an enlarged lattice spacing by a factor of  $1.29 \pm 0.1$  as compared to the cubic phase of space group Pn3m.

<sup>b</sup> $R$ , lipid-to-peptide molar ratio.

<sup>c</sup>No unequivocal phase and lattice assignment.

In the presence of GS ( $R=25$ ) the onset of Q phase formation is lowered by about 10°C as indicated by the first appearance of Bragg peaks (Fig. 5b). More interestingly, the Bragg reflections arising from the isotropic phase are less resolved as compared to the pure *A. laidlawii* B membrane polar lipids. In addition, the diffractograms for the lipid-peptide mixture are characterized by a much lower integral scattering intensity, as usually found for less ordered systems. An unequivocal assignment of the Bragg reflections in respect of a Q phase is more difficult for this microbial lipid extract in the presence of GS owing to a lack of a sufficient number of reflections allowing unambiguous assignment. Nonetheless, a Q phase of the same symmetry as found for the peptide-free lipid can be deduced from the diffractogram obtained at 25°C. The lattice spacing of 12 nm is about 1 nm smaller as compared to the pure lipid mixture (Table 1).

These X-ray diffraction data support the findings of our earlier <sup>31</sup>P-NMR experiments, where the overall axially symmetric powder pattern was shown to remain the dominant feature of the <sup>31</sup>P-NMR spectrum upon heating the *A. laidlawii* B polar lipid extract to temperatures near 90°C [9]. However, a minor sharp component centered near 2 ppm downfield was also observed, suggesting that *A. laidlawii* B polar lipid extracts form non-lamellar phases at very high temperatures. The <sup>31</sup>P-NMR spectra of the mixture of *A. laidlawii* polar lipids with GS differed significantly from those exhibited by the lipid extract alone at all temperatures above the  $L_\beta/L_\alpha$  phase transition temperature, which is in accordance with the X-ray data. Specifically, the upfield components of the <sup>31</sup>P-NMR powder patterns were considerably

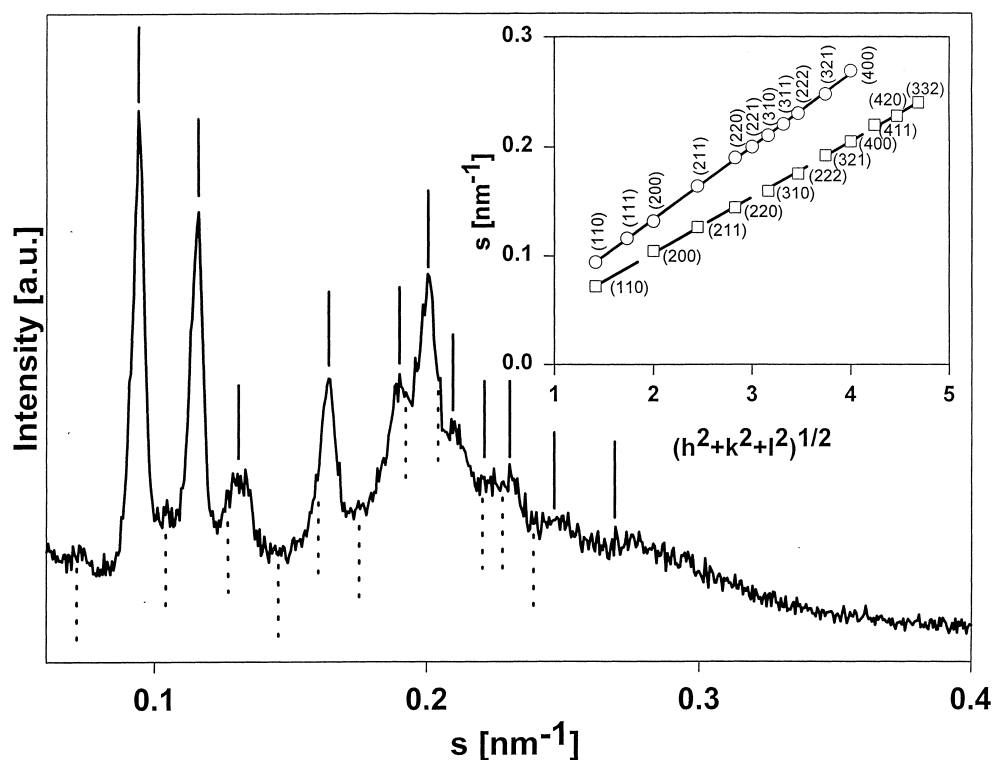


Fig. 9. Small-angle X-ray diffractogram of an aqueous dispersion of *E. coli* membrane total lipid extract recorded at 25°C after heating up the sample to 90°C;  $s$  see legend to Fig. 5. Data taken at the SAXS-beamline at the Synchrotrone ELETTRA, Trieste. Position of  $hkl$ -reflections corresponding to a cubic phase of space group Pn3m (solid line) and of space group Im3m (broken line), respectively, are indicated in the diffractogram. The inset shows the indexing of two cubic lattices from the plot  $s$  vs.  $(h^2+k^2+l^2)^{1/2}$ ; open circles represent reflections of space group Pn3m, while open squares represent reflections of space group Im3m. Miller indices ( $hkl$ ) are indicated in the panel.

sharper than observed in the absence of the peptide, and the relative intensities of the downfield components of the powder pattern were smaller than is observed with the polar lipid extract alone. Finally, at temperatures near 90°C, the major feature of the  $^{31}\text{P}$ -NMR spectrum of this lipid-GS mixture was a sharp peak centered near 2 ppm, suggesting that the interaction of GS with this particular mixture of lipids potentiates the formation of non-lamellar phases.

### 3.1. *E. coli* membrane lipid dispersions

Wide-angle X-ray diffraction patterns of polar membrane lipid extracts from *E. coli* are characterized by a diffuse reflection (data not shown), demonstrating that the hydrocarbon chains are in a melted state in the temperature range investigated (5–90°C). The small-angle X-ray data are typical for particle scattering as deduced from the broad intensive side

maxima at 6.9 nm ( $s = 0.14 \text{ nm}^{-1}$ ) and very weak side maxima at 2.1 nm ( $0.48 \text{ nm}^{-1}$ ) and 1.4 nm ( $0.71 \text{ nm}^{-1}$ ) (25°C). Above 70°C, the intensity of the side maxima decreases strongly and the onset of Bragg reflections is detectable between 85 and 90°C, which are clearly resolved upon cooling (Fig. 7a). Indexing of these Bragg reflections again revealed that the newly formed lipid structures belong to the Pn3m and Im3m space group (Fig. 8) characterized by lattice spacings of 15.3 (Table 1) and 18.3 nm, respectively. Interestingly, the (110) reflection of both Q phases exhibited similar peak intensities suggesting that in the case of *E. coli* polar lipid extract, a larger fraction of Im3m as compared to *A. laidlawii* B lipid extract does occur. Although the respective Bragg reflections increase in intensity upon cooling, broad side maxima and minima are still observed, again indicating the coexistence of a Q phase with a lamellar lipid phase. This observation is in accordance

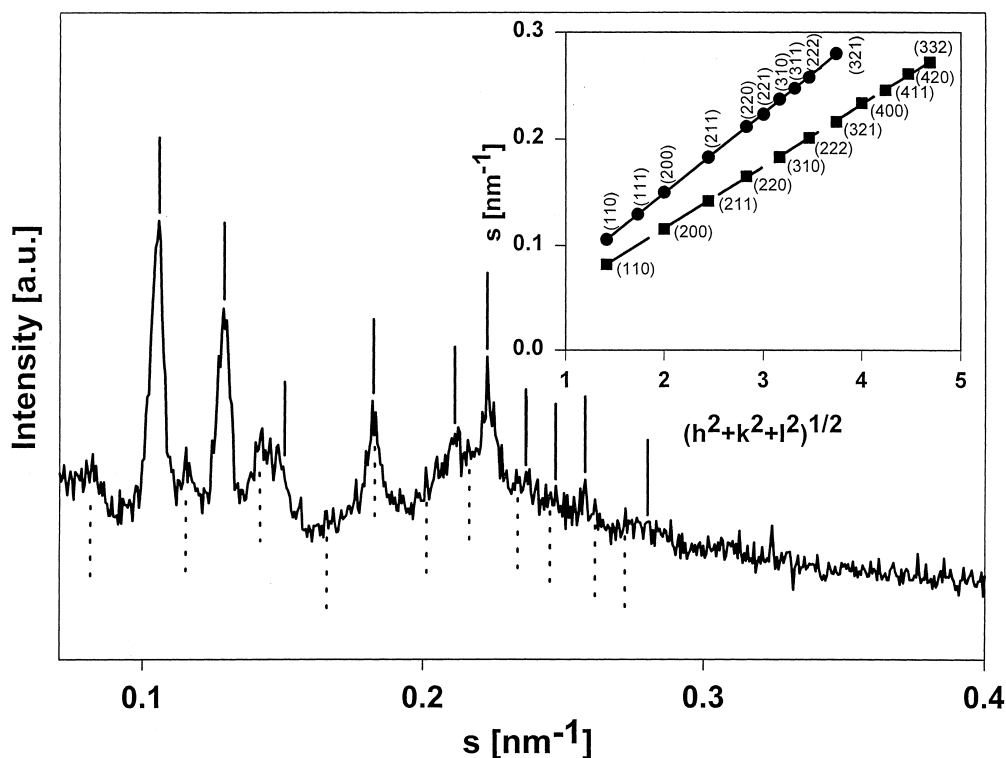


Fig. 10. Small-angle X-ray diffractogram of a mixture of *E. coli* membrane total lipid extract of these lipids with GS at a lipid-to-peptide molar ratio of 25:1 recorded at 25°C after heating up the sample to 90°C;  $s$ , see legend to Fig. 5. Data taken at the SAXS-beamline at the Synchrotrone ELETTRA, Trieste. Position of  $hkl$ -reflections corresponding to a cubic phase of space group Pn3m (solid line) and of space group Im3m (broken line), respectively, are indicated in the diffractogram. The inset shows the indexing of two cubic lattices from the plot  $s$  vs.  $(h^2+k^2+l^2)^{1/2}$ ; closed circles represent reflections of space group Pn3m, while closed squares represent reflections of space group Im3m. Miller indices ( $hkl$ ) are indicated in the panel.

with our <sup>31</sup>P-NMR data [9], showing that above 65–75°C *E. coli* lipids exhibit axially symmetric <sup>31</sup>P-NMR powder patterns typical of the lamellar liquid-crystalline phase coexisting with an isotropic component, which indicates non-lamellar phase formation.

Similar diffraction patterns were obtained for mixtures of *E. coli* membrane polar lipids and GS ( $R=25$ ) (Fig. 7b). However, the peptide decreases strongly the onset of non-lamellar phase formation by about 25°C. Phase assignment revealed the presence of the same two cubic phases as found for the pure *E. coli* polar lipid extract (Fig. 8). However, the Im3m phase represents only a minor fraction. In addition, a significant reduction of the Pn3m cubic lattice is observed in the presence of the peptide as deduced from the smaller lattice spacing parameter of 14.3 nm at 25°C after the first temperature cycling (Fig. 8, Table 1), which was less pronounced for the Im3m phase (lattice spacing of 18.0 nm). This is

again in agreement with our recent <sup>31</sup>P-NMR data, which showed a comparable decrease of the onset temperature of the non-lamellar phase formation [9]. Once formed at high temperatures, these structures form a stable and transparent gel inside the X-ray capillary. Long-lived Q phases were also reported for phosphatidylethanolamines when they were cycled through temperatures bracketing  $L_{\alpha}/H_{II}$  phase transition range [28,29]. However, the seemingly stable Q phases formed under such conditions are believed to be metastable structures which have been kinetically trapped by rapid cycling through the  $L_{\alpha}/H_{II}$  phase transition [28]. One-dimensional distance distribution functions  $p_i(r)$  were also determined for these samples to gain information on the bilayer structure. Again, as already observed for *A. laidlawii* B, the cross-bilayer distance between the phosphate groups of the opposing monolayers is diminished in the presence of the peptide from 3.9 to 3.7 nm.

Finally, the SAX pattern of aqueous dispersions of *E. coli* membrane total lipids in the presence and absence of GS closely resembled that from the polar lipid extract. For these samples, both conventional and Synchrotrone X-ray radiation experiments were carried out yielding identical results. In contrast to *E. coli* membrane polar lipids, the onset of Q phase formation was already found between 40 and 45°C, which was further reduced in the presence of the peptide. In the latter case, Bragg reflections were already observed at 25°C. Phase assignment is shown for the SAX diffraction patterns recorded from Synchrotrone experiments at 25°C after the first heating/cooling cycle using rotating X-ray capillaries (Figs. 9 and 10). The relatively large number of Bragg reflections allowed an unequivocal phase assignment (inset Figs. 9 and 10). Again it was found that the lattice spacing of the Pn3m phase decreased in the presence of GS from 14.9 to 13.4 nm (Table 1). Moreover, from these diffractograms it is evident that the coexisting Im3m phase only represents a minor fraction. Lattice spacings of 19.5 and 17.2 nm were calculated from the reciprocal gradient of  $s$  vs.  $(h^2+k^2+l^2)^{1/2}$  in the absence and presence of the peptide (inset in Figs. 9 and 10). Our results are in excellent agreement with data from Morein et al. [30] who studied lipid extracts of the inner membrane as well as an extract of the total lipids from both the inner and the outer membrane of *E. coli* and characterized their phase behavior by NMR spectroscopy. Under varying conditions, they found both H<sub>II</sub> and isotropic phase formation. Furthermore, they also investigated by X-ray diffraction the total membrane lipid extracts of *E. coli* K12 grown at 17°C and found that the isotropic phase belonged to the Pn3m space group with a lattice spacing of 14.8 nm.

#### 4. Discussion

Although the maintenance of stable lamellar structures is essential to normal membrane function, it is well known that cell membranes contain substantial quantities of so-called ‘non-lamellar’ phase-forming lipids. The importance of the proper balance between lamellar and non-lamellar phase-forming lipids has been widely discussed [31–34]. The presence of the latter significantly increases membrane monolayer

curvature stress, thereby conferring upon cell membranes a degree of non-lamellar-forming propensity. This is believed to be essential for normal membrane function (for discussions of the probable biological roles of non-lamellar phase-forming lipids, see e.g. [35–37]). The X-ray study presented here clearly demonstrates that vesicles, which are formed at room temperature from lipid extracts of the plasma membrane of *A. laidlawii* B or *E. coli*, are prone to the formation of three-dimensionally ordered structures. Specifically, inverted cubic lipid phases of the space group Pn3m and Im3m are formed upon heating the lipid extracts and, once formed, these phases persist upon cooling to physiologically relevant temperatures. Unequivocal phase assignment of cubic phases strongly depends on the number of reflections observed. This requirement was met for the Pn3m phase. On the other hand, the Im3m space group differ from the Pn3n space group only at the 11th reflection, which corresponds to the  $\sqrt{22}$  reflection of the former phase and to the  $\sqrt{21}$  reflection of the latter [38]. In the case of *A. laidlawii* B membrane lipids, this reflection could not be resolved clearly with our experimental setup. However, the lattice spacing ratio of  $1.29 \pm 0.1$  found for our systems (Table 1) is close to the value of 1.28, a theoretical value which is expected when both inverse bicontinuous cubic phases are in equilibrium in excess water [39]. The interaction of GS with these lipid extracts promotes the formation of these isotropic phases as evidenced by decreasing the temperature of the onset of this Q phase formation. The combination of X-ray diffraction (present study) and <sup>31</sup>P-NMR spectroscopic data [9] acquired with these microbial lipid extracts is consistent with the existence of a polydomain structure in which a lamellar phase coexists with a three-dimensionally ordered phase, i.e. an inverted Q phase.

A recent study has shown that alamethicin is also able to induce the formation of an inverted cubic phase of the same space group (Pn3m) in dielaidoyl PE bilayers, which coexists with the H<sub>II</sub> phase [40]. It was suggested that alamethicin may induce such phases by changing the thickness and/or flexibility of the lipid bilayer. This suggestion is supported by the observation that adsorption of alamethicin onto diphytanoyl PC bilayer causes bilayer thinning, thereby inducing chain disorder over a large area

[41,42]. Furthermore, it was shown that magainin behaves in many aspects similar to alamethicin, causing membrane thinning in PC/PS bilayers below the critical concentration for peptide insertion [43], which roughly correlates with the concentration required for cytolytic activity [44]. Very recently, Heller et al. [45] demonstrated that the  $\beta$ -sheet antimicrobial peptide protegrin-1 also decreases the thickness of diphytanoyl PC bilayers. Huang and coworkers proposed that the decrease of bilayer thickness is compensated by an increase of the hydrophobic cross-sectional area of the lipid acyl chains. This would also be consistent with the smaller cross-bilayer distances of the phosphate groups found for the GS–lipid mixtures in this study. In case of e.g. phosphatidylethanolamine, a major phospholipid component of the *E. coli* lipid extracts, this lateral expansion will further enhance the mismatch between the cross-sectional areas of the smaller, more strongly interacting headgroups and hydrocarbon side chains, inducing the lipid monolayer to curl. Although there are different molecular mechanisms that may lead to formation of non-lamellar phases by amphipathic peptides, a significant increase in monolayer curvature stress is likely to be of major importance (for review see e.g. [46,47]), and may well be key to their membrane-disruptive properties (see below). However, it is important to note that other antimicrobial peptides like magainin [48,49] or mastoparan [50], as well as hemolytic peptides, such as  $\delta$ -lysin [51], impose ‘positive’ curvature strain on non-lamellar-prone phospholipids, thereby destabilizing the bilayer structure and hence perturbing membrane integrity by different mechanisms, such as forming pores or exhibiting detergent-like action [47].

Our observations, however, clearly indicate that GS may disrupt the structural integrity of lipid membranes by promoting the formation of inverted (type II) non-lamellar lipid phases. We suggest that the limited flexibility of the  $\beta$ -turn of GS, in particular when exposed to different environmental conditions, as well as the clustered location of the ornithine side chains, might facilitate an accommodation of the peptide in the lipid membrane that favors Q phase formation. Moreover, the fact that the peptide-containing Q phases exhibit smaller lattice spacings than found for the pure lipid extracts further supports the idea that GS destabilizes the bilayer by increasing the

membrane curvature stress. A similar observation was reported from X-ray diffraction studies, which showed that the lattice parameter of the inverse hexagonal phase in the presence of the fusion peptide of simian immunodeficiency virus (SIV) was slightly less as compared to the peptide-free lipid system [52]. These authors demonstrated that peptides resembling the N-terminus of the SIV fusion peptide only exhibited fusogenic activity when capable of inducing negative curvature stress in a set of three different PE matrices. In contrast, a peptide of the same amino acid composition, but an altered sequence, induced positive curvature stress and was thus not fusogenic. In addition, a variety of amphiphilic peptides or proteins that raised the  $L_{\alpha}/H_{II}$  phase transition temperature were shown to be inhibitors of viral fusion [53]. The potential of GS to facilitate or induce phase changes that can lead to fusion was described by Legendre and Szoka [54], who showed that a 1:1 complex of GS and DNA was mixed with a  $H_{II}$  phase-competent phosphatidylethanolamine and successfully used for cell transfection [55,56]. The active involvement of transient lipid rearrangements in membrane fusion was previously proposed by Siegel [57,58]. These observations are in agreement with data described and discussed in this paper and offer intriguing interpretations for the biological activity of GS.

That the membrane-disrupting capacity of GS may actually be a function of the non-lamellar phase-forming propensity of the target cell membrane has some interesting implications for the mechanism of action of this peptide. The non-lamellar-forming propensities of lipid bilayers are largely determined by their monolayer curvature stress [59,60], which in our case will be different for each lipid or mixtures thereof. Nevertheless, given that GS promotes the formation of highly curved structures, such as Q phases when it interacts with lipid bilayers, we can conclude that the monolayer curvature stress in bilayers derived from lipid–GS mixtures significantly exceeds that which occurs in the corresponding peptide-free membrane. We suggest that the occurrence of localized domains of high curvature stress are probably key to the cytolytic activities of GS. This is because defects occurring at the boundaries of these domains may function as sites through which the leakage of cellular contents may either occur. Moreover, be-

cause of the localized effects of such lipid–peptide interaction, these defects may begin to accumulate at low peptide-to-lipid molar ratios and will be maximal when the intrinsic monolayer curvature stress of the membrane is high or when large disparities between the curvature stresses in peptide-rich and peptide-poor membrane domains exist. Therefore, one can envisage how the degradation of membrane barrier properties and other forms of membrane destabilization can readily occur once the number of such defects exceeds some critical value.

Previous work has also shown that GS promotes the release of small phospholipid particles from *E. coli* and it was suggested that this process may be responsible for the leakage of intracellular components and, ultimately, cell death [61–63]. It was also demonstrated that marked changes in cell morphology occur when GS binds to the erythrocyte membrane [62]. The results of these studies are all compatible with our suggestion of GS induced membrane destabilization being mediated by highly localized domains of high membrane monolayer curvature stress. Another aspect of this suggestion is that the probability of significant peptide-induced membrane disruption should increase with the increases in the intrinsic curvature stress of the membrane. Since significant amounts of non-lamellar phase-forming lipids are present in virtually all cell membranes, it follows that all membranes should be susceptible to disruption by GS, though their susceptibility to its action should vary with amount of non-lamellar phase-forming lipids present as well as their intrinsic non-lamellar-forming propensity.

In conclusion, our data suggests that GS has considerable potential for destabilizing lipid bilayers with respect to highly curved and/or inverted non-lamellar phases. It should also be noted that unlike mammalian membranes, glycolipids are the predominant structural components of *A. laidlawii* B membranes. Interestingly, the first micellar-preferring bacterial membrane lipid has also been described in this mycoplasma, namely glycerylphosphoryldiglucoyl-diacylglycerol [64]. Diglucoyldiacylglycerol and phosphatidylglycerol, the other major lipid component of the *A. laidlawii* B membrane, were shown to form only lamellar phases in the temperature range of 5–80°C, whereas monoglucoyldiacylglycerol exists in a lamellar phase at lower temperatures,

but does form non-lamellar phases at higher temperatures [25,26,33]. The finding from a recent monolayer study, that the lipid mixture of *A. laidlawii* A pack more closely than the individual components, further emphasizes the capability of such lipid mixtures to form non-lamellar structures owing to supposedly increased hydrogen bonding between the polar head group of PG and the sugar groups of the glycolipids [65]. While FTIR data suggest moderate interaction of GS with single glycolipids [66], stronger interaction with phosphatidylglycerol has been reported [67]. Nevertheless, the demonstration that GS can promote the formation of non-lamellar phases in these membranes indicates that this property is not limited to phospholipid-based lipid bilayers. We note that the suggestion that the cytolytic activities of GS may actually be directed at the non-lamellar phase-forming tendencies of its membrane targets does not rule out the possibility that electrostatic interactions between the basic residues of GS and the negatively charged phosphate groups of phospholipid molecules may initiate or otherwise facilitate lipid–GS interactions. The basic residues of GS seem to be intimately linked to its antimicrobial activity (see [2,5,68,69]) and negatively charged lipids form a significant fraction of virtually all bacterial cell membranes. Thus, it seems likely that at the very least, electrostatic interactions between the basic residues of GS and negatively charged moieties at the surfaces of cell membranes may promote antibiotic activity through the kinetic facilitation of lipid–peptide interaction. Moreover, we have recently shown that the presence of cholesterol reduces the interactions of GS with PC model membranes and reduces the propensity of GS to induce inverted non-lamellar phases in PE model membranes [70]. We also note that the mechanism proposed above neither implies nor requires the actual formation of cubic phases under the conditions where the cytolytic activity of GS is commonly observed. The amount of GS required in our experiments to detect significant Q phase formation may exceed that which was reported for antibiotic and hemolytic activities (for examples of the latter, see [4,5] and references cited therein). However, the formation of Q phases or other three-dimensionally ordered structures can provide valuable information about the general mechanism of action of this antimicrobial peptide. This, in turn, may

be helpful for the development of more specific and potent GS derivatives.

### Acknowledgements

This work was supported by a National Grant of the Austrian Ministry of Science and Transportation (K.L.) as well as from the Jubiläumsfonds der Österreichischen Nationalbank (Project 7190, K.L.) and by an operating grant from the Medical Research Council of Canada and the Protein Engineering Network of Centers of Excellence (R.N.M.), and by a postdoctoral fellowship to E.J.P. from the Alberta Heritage Foundation for Medical Research. The authors are indebted to Dr. Heinz Amenitsch for his technical assistance with the Synchrotrone experiments at ELETTRA, Trieste, Italy.

### References

- [1] G.F. Gause, M.G. Brazhnikova, Gramicidin S and its use in the treatment of infected wounds, *Nature* 154 (1944) 703.
- [2] N. Izumiya, T. Kato, H. Aoyaga, M. Waki, M. Kondo (Eds.), Relationship between the primary structure and activity of gramicidin S and tyrocidines, in: *Synthetic Aspects of Biologically Active Cyclic Peptides: Gramicidin S and Tyrocidines*, Halsted Press, New York, 1979, pp. 49–70.
- [3] M. Waki, N. Izumiya, Recent advances in the biotechnology of  $\beta$ -lactams and microbial bioactive peptides, in: H. Kleinhau, H. van Doren (Eds.), *Biochemistry of Peptide Antibiotics*, de Gruyter, Berlin, 1990, pp. 205–244.
- [4] L.H. Kondejewski, S.W. Farmer, D.S. Wishart, C.M. Kay, R.E.W. Hancock, R.S. Hodges, Gramicidin S is active against both Gram-positive and Gram-negative bacteria, *Int. J. Pept. Protein Res.* 47 (1996) 460–466.
- [5] L.H. Kondejewski, S.W. Farmer, D.S. Wishart, C.M. Kay, R.E.W. Hancock, R.S. Hodges, Modulation of structure and antibacterial and hemolytic activity by ring size in cyclic gramicidin S analogs, *J. Biol. Chem.* 271 (1996) 25261–25268.
- [6] R. Schwyzler, in: *Amino Acids and Peptides with Antimetabolic Activity*, Churchill, New York, 1958, p. 171.
- [7] T. Kato, N. Izumiya, Conformations of di-*N*-methylleucine gramicidin S and *N*-methylleucine gramicidin S compatible with the sidedness hypothesis, *Biochim. Biophys. Acta* 493 (1977) 235–238.
- [8] E.J. Prenner, R.N.A.H. Lewis, R.N. McElhaney, The interaction of the antimicrobial peptide gramicidin S with lipid bilayer model and biological membranes, *Biochim. Biophys. Acta* 1462 (1999) 201–221.
- [9] E.J. Prenner, R.N.A.H. Lewis, K.C. Neuman, S.M. Gruner, L.H. Kondejewski, R.S. Hodges, R.N. McElhaney, Nonlamellar phases induced by the interaction of gramicidin S with lipid bilayers. A possible relationship to membrane-disrupting activity, *Biochemistry* 36 (1997) 7906–7916.
- [10] J. Seelig,  $^{31}\text{P}$  Nuclear magnetic resonance and the headgroup structure of phospholipid membranes, *Biochim. Biophys. Acta* 515 (1978) 105–140.
- [11] C.P.S. Tilcock, P.R. Cullis, S.M. Gruner, On the validity of  $^{31}\text{P}$ -NMR determinations of phospholipid polymorphic phase behavior, *Chem. Phys. Lipids* 40 (1986) 47–56.
- [12] J.R. Silvius, N. Mak, R.N. McElhaney, Lipid and protein composition and thermotropic lipid phase transitions in fatty acid-homogeneous membranes of *Acholeplasma laidlawii* B, *Biochim. Biophys. Acta* 597 (1980) 199–215.
- [13] P. Laggner, H. Mio, SWAX – a dual detector camera for simultaneous small- and wide-angle X-ray diffraction in polymer and liquid crystal research, *Nucl. Inst. Methods Phys. Res. A* 323 (1992) 86–90.
- [14] H. Amenitsch, S. Bernstorff, M. Kriechbaum, D. Lombardo, H. Mio, M. Rappolt, P. Laggner, Performance and First results of the ELETTRA high-flux beamline for small-angle X-ray scattering, *J. Appl. Crystallogr.* 30 (1997) 872–876.
- [15] O. Glatter, A new method for the evaluation of small-angle scattering data, *J. Appl. Crystallogr.* 10 (1977) 415–421.
- [16] O. Glatter, Data Treatment, in: O. Glatter, O. Kratky (Eds.), *Small Angle X-Ray Scattering*, Academic Press, London, 1982, pp. 119–166.
- [17] O. Glatter, Interpretation, in: O. Glatter, O. Kratky (Eds.), *Small Angle X-Ray Scattering*, Academic Press, London, 1982, pp. 167–196.
- [18] A. Tardieu, V. Luzatti, F.C. Reman, Structure and polymorphism of the hydrocarbon chains of lipids: a study of lecithin–water phases, *J. Mol. Biol.* 75 (1973) 711–733.
- [19] J.A. Bouwstra, G.S. Gooris, W. Bras, H. Talsma, Small angle X-ray scattering: possibilities and limitations in characterization of vesicles, *Chem. Phys. Lipids* 64 (1993) 83–98.
- [20] A.E. Blaurock, Evidence of bilayer structure and of membrane interactions from X-ray diffraction analysis, *Biochim. Biophys. Acta* 650 (1982) 167–207.
- [21] J.M. Seddon, Structure of the inverted hexagonal ( $\text{H}_{\text{II}}$ ) phase, and non-lamellar phase transitions of lipids, *Biochim. Biophys. Acta* 1031 (1990) 1–69.
- [22] S.M. Gruner, M.W. Tate, G.L. Kirk, P.T. So, D.C. Turner, D.T. Keane, X-ray diffraction study of the polymorphic behavior of *N*-methylated dioleoylphosphatidylethanolamine, *Biochemistry* 27 (1988) 2853–2866.
- [23] J. Erbes, C. Czeslik, W. Hahn, R. Winter, M. Rappolt, G. Rapp, On the existence of bicontinuous cubic phases in dioleoylphosphatidylethanolamine, *Ber. Bunsenges. Phys. Chem.* 98 (1994) 1287–1293.
- [24] B. Tenchov, R. Koynova, G. Rapp, Accelerated formation of cubic phases in phosphatidylethanolamine dispersions, *Biophys. J.* 75 (1998) 853–866.
- [25] A. Sen, S.W. Hui, D.A. Mannock, R.N.A.H. Lewis, R.N. McElhaney, Physical properties of glycosyl diacylglycerols.

2. X-ray diffraction studies of a homologous series of 1,2-di-O-acyl-3-O-( $\alpha$ -D-glucopyranosyl)-sn-glycerols, *Biochemistry* 29 (1990) 7799–7804.
- [26] A.-S. Andersson, L. Rilfors, G. Orädd, G. Lindblom, Total lipids with short and long acyl chains from *Acholeplasma* form nonlamellar phases, *Biophys. J.* 75 (1998) 2877–2887.
- [27] G. Lindblom, L. Rilfors, Cubic phases and isotropic structures formed by membrane lipids – possible biological significance, *Biochim. Biophys. Acta* 988 (1989) 221–256.
- [28] E. Shyamsunder, S.M. Gruner, M.W. Tate, D.C. Turner, P.T.C. So, C.P.S. Tilcock, Observation of inverted cubic phase in hydrated dioleoylphosphatidylethanolamine membranes, *Biochemistry* 27 (1988) 2332–2336.
- [29] J.A. Veiro, R.G. Khalifah, E.S. Rowe, P-31 nuclear magnetic resonance studies of the appearance of an isotropic component in dielaidoylphosphatidylethanolamine, *Biophys. J.* 57 (1990) 637–641.
- [30] S. Morein, A.-S. Andersson, L. Rilfors, G. Lindblom, Wild-type *Escherichia coli* cells regulate the membrane lipid composition in a ‘window’ between gel and non-lamellar structures, *J. Biol. Chem.* 271 (1996) 6801–6809.
- [31] L. Rilfors, G. Lindblom, A. Wieslander, A. Christiansson, Membrane Fluidity, in: M. Kates, L.A. Mason (Eds.), *Biomembranes*, Vol. 12, Plenum Press, New York, 1984, pp. 205–245.
- [32] L. Rilfors, A. Wieslander, G. Lindblom, Regulation and physicochemical properties of the polar lipids in *Acholeplasma laidlawii*, in: S. Rottem, I. Kahane (Eds.), *Subcellular Biochemistry*, Vol. 20, Plenum Press, New York, 1993, pp. 109–166.
- [33] P.J. Foht, Q.M. Tran, R.N.A.H. Lewis, R.N. McElhaney, Quantitation of the phase preferences of the major lipids of the *Acholeplasma laidlawii* B membrane, *Biochemistry* 34 (1995) 13811–13817.
- [34] R.N. McElhaney, in: J. Maniloff, R.N. McElhaney, L.R. Finch, J.B. Baseman (Eds.), *Mycoplasma: Molecular Biology and Pathogenesis*, American Society for Microbiology, Washington, DC, 1992, pp. 113–155.
- [35] S.-W. Hui, A. Sen, Effects of lipid packing on polymorphic phase behavior and membrane properties, *Proc. Natl. Acad. Sci. USA* 86 (1989) 5825–5829.
- [36] S.M. Gruner, Non-lamellar lipid phases, in: P.L. Yeagle (Ed.), *Structure of Biological Membranes*, CRC Press, Boca Raton, FL, 1992, pp. 211–250.
- [37] K. Lohner, Is the high propensity of ethanolamine plasmalogen to form non-lamellar lipid structures manifested in the properties of biomembranes?, *Chem. Phys. Lipids* 81 (1996) 167–184.
- [38] J.S. Kasper, K. Lonsdale, *International Tables for X-ray Crystallography*, Vol. 2, Riedel, Dordrecht, 1985.
- [39] S. Hyde, S. Andersson, B. Ericsson, K. Larsson, A cubic structure consisting of a lipid bilayer forming an infinite periodic minimum surface of the gyroid type in the glyceromonoleate–water system, *Z. Kristallogr.* 168 (1984) 213–219.
- [40] S.L. Keller, S.M. Gruner, K. Gawrisch, Small concentrations of alamethicin induce a cubic phase in bulk phosphatidylethanolamine mixtures, *Biochim. Biophys. Acta* 1127 (1996) 241–246.
- [41] Y. Wu, K. He, S.J. Ludtke, H.W. Huang, X-ray diffraction study of lipid bilayer membranes interacting with amphiphilic helical peptides: diphytanoyl phosphatidylcholine with alamethicin at low concentrations, *Biophys. J.* 68 (1995) 2361–2369.
- [42] K. He, S.J. Ludtke, W.T. Heller, H.W. Huang, Mechanism of alamethicin insertion into lipid bilayers, *Biophys. J.* 71 (1996) 2669–2897.
- [43] S.J. Ludtke, K. He, H.W. Huang, Membrane thinning caused by magainin 2, *Biochemistry* 34 (1995) 16764–16769.
- [44] S.J. Ludtke, K. He, Y. Wu, H.W. Huang, Cooperative membrane insertion of magainin correlated with its cytolytic activity, *Biochim. Biophys. Acta* 1190 (1994) 181–184.
- [45] W.T. Heller, A.J. Waring, R.I. Lehrer, T.A. Harroun, T.M. Weiss, L. Yang, H.W. Huang, Membrane thinning effect of the beta-sheet antimicrobial protegrin, *Biochemistry* 39 (2000) 139–145.
- [46] R.M. Epand, Lipid polymorphism and protein–lipid interactions, *Biochim. Biophys. Acta* 1376 (1998) 353–368.
- [47] K. Lohner, E.J. Prenner, Differential scanning calorimetry and X-ray diffraction studies of the specificity of the interaction of antimicrobial peptides with membrane-mimetic systems, *Biochim. Biophys. Acta* 1462 (1999) 141–156.
- [48] T. Wieprecht, M. Dathe, R.M. Epand, M. Beyermann, E. Krause, W.L. Maloy, D.L. MacDonald, M. Bienert, Influence of the angle subtended by the positively charged helix face on the membrane activity of amphipathic, antibacterial peptides, *Biochemistry* 36 (1997) 12869–12880.
- [49] K. Matsuzaki, K. Sugishita, N. Ishibe, M. Ueha, S. Nakata, K. Miyajima, R.M. Epand, Relationship of membrane curvature to the formation of pores by magainin 2, *Biochemistry* 37 (1998) 11856–11863.
- [50] E.M. Tytler, J.P. Segrest, R.M. Epand, S.-Q. Nie, R.F. Epand, V.K. Mishra, Y.V. Venkatachalapathi, G.M. Anantharamaiah, Reciprocal effects of apolipoprotein and lytic peptide analogs on membranes – cross-sectional molecular shapes of amphipathic alpha helices control membrane stability, *J. Biol. Chem.* 268 (1993) 22112–22118.
- [51] E. Staudegger, Interaction of the Hemolytic Bacteriotoxin  $\delta$ -Lysin with Model Membranes, Thesis, 1998, Graz University of Technology.
- [52] A. Colotto, I. Martin, J. Ruyschaert, A. Sen, S.W. Hui, R.M. Epand, Structural study of the interaction between the SIV fusion peptide and model membranes, *Biochemistry* 35 (1996) 980–989.
- [53] R.M. Epand, in: R.C. Aloia, C.C. Curtain (Eds.), *Membrane Interactions of HIV: Implications for Pathogenesis and Therapy in Aids*, Wiley-Liss, New York, 1992, pp. 99–112.
- [54] J.Y. Legendre, F.C. Szoka, Cyclic amphipathic peptide-DNA complexes mediate high-efficiency transfection of adherent mammalian cells, *Proc. Natl. Acad. Sci. USA* 90 (1993) 893–897.

- [55] J.Y. Legendre, A. Supersaxo, Short-chain phospholipids enhance amphipathic peptide-mediated gene transfer, *Biochem. Biophys. Res. Commun.* 217 (1995) 179–185.
- [56] T. Hara, H. Kuwasawa, Y. Aramaki, S. Takada, K. Koike, K. Ishidate, H. Kato, S. Tsuchiya, Effects of fusogenic and DNA-binding amphiphilic compounds on the receptor-mediated gene transfer into hepatic cells by asialofetuin-labeled liposomes, *Biochim. Biophys. Acta* 1278 (1996) 51–58.
- [57] D.P. Siegel, Energetics of intermediates in membrane fusion: comparison of stalk and inverted micellar intermediate mechanisms, *Biophys. J.* 65 (1993) 2124–2140.
- [58] D.P. Siegel, The modified stalk mechanism of lamellar/inverted phase transitions and its implications for membrane fusion, *Biophys. J.* 76 (1999) 291–313.
- [59] G.L. Kirk, S.M. Gruner, D.E. Stein, A thermodynamic model of the lamellar ( $L_{\alpha}$ ) to inverse hexagonal ( $H_{II}$ ) lipid membrane–water systems, *Biochemistry* 23 (1984) 1093–1102.
- [60] S.M. Gruner, Intrinsic curvature hypothesis for biomembrane lipid composition: a role for nonbilayer lipids, *Proc. Natl. Acad. Sci. USA* 82 (1985) 3665–3669.
- [61] T. Katsu, H. Kobayashi, Y. Fujita, Mode of action of gramicidin S on *Escherichia coli* membrane, *Biochim. Biophys. Acta* 860 (1986) 608–619.
- [62] T. Katsu, C. Ninomiya, M. Kuroko, H. Kobayashi, T. Hirata, Y. Fujita, Action mechanism of amphipathic peptides gramicidin S and melittin on erythrocyte membrane, *Biochim. Biophys. Acta* 939 (1988) 57–63.
- [63] T. Katsu, M. Kuroko, T. Morikawa, K. Sanchicka, Y. Fujita, H. Yamamura, M. Uda, Mechanism of membrane damage induced by the amphipathic peptides gramicidin S and melittin, *Biochim. Biophys. Acta* 983 (1989) 135–141.
- [64] R.N.A.H. Lewis, R.N. McElhaney, *Acholeplasma laidlawii* B membranes contain a lipid (glycerylphosphoryldiglucoyl-diacylglycerol) which forms micelles rather than lamellar or reversed phases when dispersed in water, *Biochemistry* 34 (1995) 13818–13824.
- [65] A.-S. Andersson, R.A. Demel, L. Rilfors, G. Lindblom, Lipids in total extracts from *Acholeplasma laidlawii* A pack more closely than the individual lipids. Monolayers studied at the air–water interface, *Biochim. Biophys. Acta* 1369 (1998) 94–102.
- [66] R.N.A.H. Lewis, E.J. Prenner, L.H. Kondejewski, C.R. Flach, R. Mendelsohn, R.S. Hodges, R.N. McElhaney, Fourier transform infrared spectroscopic studies of the interaction of the antimicrobial peptide gramicidin S with lipid micelles and with lipid monolayer and bilayer membranes, *Biochemistry* 38 (1999) 15193–15203.
- [67] E.J. Prenner, R.N.A.H. Lewis, L.H. Kondejewski, R.S. Hodges, R.N. McElhaney, Differential scanning calorimetric study of the effect of the antimicrobial peptide gramicidin S on the thermotropic phase behavior of phosphatidylcholine, phosphatidylethanolamine and phosphatidylglycerol lipid bilayer membranes, *Biochim. Biophys. Acta* 1417 (1999) 211–223.
- [68] Y.A. Ovchinnikov, V.T. Ivanov, Conformational states and biological activity of cyclic peptides, *Tetrahedron* 31 (1975) 2177–2209.
- [69] Y.A. Ovchinnikov, V.T. Ivanov, The cyclic peptides: structure, conformation, and function, in: H. Neurath, R.L. Hill (Eds.), *The Proteins*, Vol. V, Academic Press, New York, 1982, pp. 391–398.
- [70] E.J. Prenner, R.N.A.H. Lewis, M. Jelokhani-Niaraki, R.S. Hodges, R.N. McElhaney, Cholesterol attenuates the interaction of the antimicrobial peptide gramicidin S with phospholipid bilayer membranes, *Biochim. Biophys. Acta*, submitted for publication.